END
DATE
FILMED
5 82
DTIC

MICROCOPY RESOLUTION TEST CHART
NATIONAL BUREAU OF STANDARDS 1963 A

| REPORT DOCUMENTATION PAGE | | READ INSTRUCTIONS BEFORE COMPLETING FORM |
|---|---|---|
| **1. REPORT NUMBER** R-1527 | **2. GOVT ACCESSION NO.** AD+A113497 | **3. RECIPIENT'S CATALOG NUMBER** |
| **4. TITLE** *(and Subtitle)* MATERIALS RESEARCH FOR ADVANCED INERTIAL INSTRUMENTATION; TASK 1: DIMENSIONAL STABILITY OF GYROSCOPE STRUCTURAL MATERIALS (Technical Report No. 4) | | **5. TYPE OF REPORT & PERIOD COVERED** Research Report 10/1/80 – 9/30/81 |
| | | **6. PERFORMING ORG. REPORT NUMBER** R-1527 |
| **7. AUTHOR(s)** K. Kumar, F. Petri, and J. Wollam | | **8. CONTRACT OR GRANT NUMBER(s)** N00014-77-C-0388 |
| **9. PERFORMING ORGANIZATION NAME AND ADDRESS** The Charles Stark Draper Laboratory, Inc. 555 Technology Square Cambridge, Massachusetts 02139 | | **10. PROGRAM ELEMENT, PROJECT, TASK AREA & WORK UNIT NUMBERS** |
| **11. CONTROLLING OFFICE NAME AND ADDRESS** Office of Naval Research Department of the Navy 800 N. Quincy St., Arlington, Virginia 20217 | | **12. REPORT DATE** December 1981 |
| | | **13. NUMBER OF PAGES** 48 |
| **14. MONITORING AGENCY NAME & ADDRESS** *(if different from Controlling Office)* Office of Naval Research Boston Branch, Bldg. 114, Sec. D 666 Summer Street Boston, Massachusetts 02210 | | **15. SECURITY CLASS.** *(of this report)* Unclassified |
| | | **15a. DECLASSIFICATION/DOWNGRADING SCHEDULE** |

**16. DISTRIBUTION STATEMENT** *(of this Report)*

Approved for public release, distribution unlimited.

**17. DISTRIBUTION STATEMENT** *(of the abstract entered in Block 20, if different from Report)*

**18. SUPPLEMENTARY NOTES**

**19. KEY WORDS** *(Continue on reverse side if necessary and identify by block number)*

| | |
|---|---|
| Dimensional Stability | Microcreep |
| Finite Element Analysis | Micromechanical Properties |
| Gyroscope Materials | Microstrain Modeling |
| Hot Isostatically Pressed Beryllium | Microyield Strength |
| X-520 Beryllium | Optical and Electron Microscopy |

**20. ABSTRACT** *(Continue on reverse side if necessary and identify by block number)*

Macroyield experiments were performed on HIP-50 beryllium samples. These samples had been investigated for their microyield behavior during the last reporting period. Micro- as well as macroyield experiments were also performed on as-received and heat treated samples of the X-520 grade of beryllium and these results were compared with those obtained on HIP-50.

(continued)

**DD** FORM 1 JAN 73 **1473** EDITION OF 1 NOV 65 IS OBSOLETE

Significant differences were observed for these two beryllium grades with respect to their "micro" properties, even though their "macro" properties were quite comparable. The microyield strength (MYS) values for as-received and heat treated HIP-50 samples were in the range of 17 to 27 kpsi; those for similarly heat treated X-520 samples, however, ranged only from about 8 to 9 kpsi. Differences were also noted in the value of the strain exponent, which was measured as the slope of the line generated by plotting the stress versus residual plastic strain data on logarithmic coordinates. Strain exponent values of 0.20 to 0.34 were observed for the HIP-50 data compared to the range of 0.38 to 0.48 observed for the X-520 data.

Scanning electron microscopy (SEM) observations on fractured surfaces of the several samples failed to show many topographical differences between HIP-50 and X-520. A few regions in the X-520 material, however, appeared less crystalline than the surrounding material. X-ray mapping of these regions in the SEM showed higher quantities of Si, O, and Al in these regions. Subsequent X-ray diffraction examination of these materials showed the presence of a few extra peaks in the patterns obtained from the X-520 samples which were noticeably absent in the HIP-50 diffraction data. These extra peaks were attributed to the presence of $Be_2SiO_4$ as an extraneous phase in the X-520 material. Further electron microscopic examination of the X-520 samples is planned.

A reasonably extensive effort was expended on the design of an experimental piece of apparatus for measuring microcreep at the $10^{-7}$ inch/inch level. The system has been designed to accommodate the application of load in the range of 100 to 10,000 psi with test runs that will allow sample temperature to be maintained at a given value between 100 and 180 $^\circ$F, regulated to within $\pm 0.02 ^\circ$F. Strain will be measured using a capacitance probe specially designed for this purpose.

| Accession For | | |
|---|---|---|
| NTIS GRA&I | | ☒ |
| DTIC TAB | | ☐ |
| Unannounced | | ☐ |
| Justification | | |
| By | | |
| Distribution/ | | |
| Availability Codes | | |
| Dist | Avail and/or Special | |
| A | | |

DTIC
COPY
INSPECTED
2

R-1527


MATERIALS RESEARCH FOR ADVANCED INERTIAL INSTRUMENTATION


TASK 1: DIMENSIONAL STABILITY OF GYROSCOPE STRUCTURAL MATERIALS


DECEMBER 1981


TECHNICAL REPORT NO. 4


FOR THE PERIOD

1 October 1980 - 30 September 1981


K. Kumar, F. Petri, J. Wollam

Approved: _____

M.S. Sapuppo, Head
Component Development Department


The Charles Stark Draper Laboratory
Cambridge, Massachusetts  02139

# ACKNOWLEDGEMENTS

TABLE OF CONTENTS

## LIST OF ILLUSTRATIONS

## LIST OF TABLES

# SECTION 1

## INTRODUCTION

Structural members of inertial instruments undergo dimensional changes from micromechanical processes during different modes of assembly and operation.  These changes manifest themselves in small amounts of mass shifts which become sources of error in the performance of the inertial devices.  The sources of dimensional instability are several among which some readily identifiable ones are phase transformation, relief of residual stresses, and microplastic deformation occurring because of externally applied stresses.  These externally applied stresses are the most difficult to control in that some minimum elastic stresses need to be applied to the different structural members when the instrument is assembled for satisfactory functioning of the instrument with high physical integrity.  The gradual relief of such applied elastic stresses, with the passage of time, results in permanent shape changes in the material (giving rise to mass shifts) because of the induced plastic strain.  Dimensional changes occurring from effects such as phase transformations and relief of residual stresses, on the other hand, can be substantially minimized (if not altogether eliminated) by appropriate material and process selection procedures.

Ideally, advanced generations of inertial instruments require that induced long-term microplastic strains be maintained at levels substantially lower than $10^{-6}$ to $10^{-7}$ inch/inch.  Strains of this low order of magnitude can result in moderate strength engineering materials with the application of very low applied stresses such as those that are associated with essential assembly operations such as shrink fit, bolt tension, or rotational stress.  Because it is not possible to reduce these stresses below a reasonable limit, it becomes desirable to predict the plastic microstrain in such circumstances and compensate for the resulting errors.  In the past, much of the prediction criteria for the

1

several instrument component members has been based on the use of the measured microyield strength (MYS) of the material. (A microyield strength measurement typically consists of a series of short-term load-unload cycles, increasing in stress level. During this period the total accumulated residual plastic strain is recorded for each incrementally higher level of applied stress. Conventionally, that level of applied stress which is required to result in one residual microstrain (= $10^{-6}$ strain) is referred to as the microyield strength of the material). More recently, however, it has become apparent that microcreep, which is a continuous dimensional change measured at a $10^{-6}$ or lower strain level at a given temperature and applied load, is of considerably more significance to the designer than is the MYS of the material which appears only suited to short-term strain effects.[1] Observations elsewhere[2] have shown that significant microcreep will occur at stress levels that are but only a fraction of the measured MYS value.

The emphasis in this activity has progressively shifted from a determination of the MYS value of the HIP-50 beryllium material to an examination of other experimental grades of beryllium. In particular, the X-520 grade of beryllium produced by the Brush-Wellman Co. has been examined for MYS in a manner analogous to the HIP-50 Be. Attempts are also underway to fabricate and assemble an apparatus capable of measuring long-term microcreep at strain levels on the order of $10^{-7}$ inch/inch. A close examination of the microstructure of the several beryllium samples using standard analytical techniques has continued with the aim of eventually being able to explain the effects of selected heat treatments on the measured micromechanical properties of the different grades of beryllium. The efforts are also aimed at developing finite element modelling techniques for predicting actual material behavior from the measured rates of microcreep. Efforts have recently been initiated towards the procurement of metal matrix composite materials for evaluation as alternate materials to beryllium.

SECTION 2

OBJECTIVES

The present objectives of this program are as follows:

(1)   To survey the literature on microplastic properties of
       materials and summarize the data for use in modelling
       instrument performance and design analysis.   [This
       information was contained in reference (3).]

(2)   To study the microplastic behavior of HIP-50 and X-520
       grades of beryllium and the relationship to microstructure.

(3)   To predict microdeformation behavior of typical instrument
       component￼   ,ing finite element analysis techniques and
       experimentally determined microcreep data.

(4)   To investigate the suitability of metal-matrix composite
       materials as alternate materials to beryllium as the
       structural members of the inertial devices.

# SECTION 3

## PREVIOUS WORK

Work accomplished prior to this past year's effort is described in detail in references (1,), (3), and (4). A brief summary is included here.

(1) Procedures were established for preparing specimens and measuring values of their microyield strength (MYS) while ensuring that a reasonable precision of alignment was obtained.

(2) MYS measurements were performed on as-received and heat treated hot isostatically pressed HIP-50 beryllium purchased from Kawecki Berylco Industries. The highest MYS value of 26.5 kpsi was obtained after heat treating the as-received material at 600°C for 100 hours.

(3) The HIP-50 MYS measurements showed that if a correlation is desired between the processes of microyield and microcreep one must take into account the value of the strain exponent in the low strain regime (obtained by plotting the data on logarithmic coordinates) in addition to the measured MYS value.

(4) Optical microscopy was determined to be of limited utility in determining the effects of the several thermal treatments on sample microstructure. However, it was concluded that extreme care was needed in sample preparation for microstructure examination to avoid introducing damage in regions near the surface.

(5) Transmission electron microscopy was determined to be a
substantially more powerful tool for examining sample
microstructure. Initial examinations of the as-HIPed
material was made at the National Bureau of Standards using
a perchloric based solution.[4] Subsequent examinations
were performed on heat treated HIP-50 samples at a local
facility using a chromic-acetic solution which was
successfully investigated for this purpose. The differences
noted in the samples were related mainly to phase
precipitation and segregation.

(6) Modelling studies were performed on a typical gyro component
and on a disc-shaped specimen for biaxial loading.
Deflection, resulting from microcreep processes, were
calculated for these instances. Finite element analytical
techniques were also extended for evaluating the stress
field in a proposed test specimen for microcreep
measurements. It was determined that if three individual
lugs were used to replace the axisymmetric ribs of a
conventional tensile microcreep sample, a substantially more
uniform stress field is obtained.

# SECTION 4

## PRESENT WORK

Progress achieved during this past year was mainly related to experimental determination of the microyield ($10^{-6}$ strain) and macroyield (0.2 percent strain) properties of the X-520 grade of beryllium, their comparison with similar data on HIP-50 beryllium, interpretation of the measured mechanical properties with respect to sample microstructure, and use of the finite element analysis technique for predicting the microdeformation behavior of typical instrument components from the experimentally obtained microcreep data. Most of this data is currently being collected on I-400 grade of beryllium at the National Bureau of Standards (NBS) under a parallel program which is also supported by the Office of Naval Research. (The Charles Stark Draper Laboratory, Inc., serves as a source of applications information to NBS and has provided this past year [as in previous years] the specialized beryllium machining facilities for manufacturing the microcreep specimens.)

### 4.1 Physical and Chemical Property Differences between the Different Grades of Beryllium

There are significant structure, fabrication process, and chemical composition differences between the different grades of beryllium currently under investigation at CSDL and NBS. The rationale for examining these different beryllium grades arises from the recognition that the several differences that exist must somehow influence the mechanical (microyield and microcreep) properties that are measured. The large data base that these different beryllium grades provide should ultimately aid in the establishment of a detailed, high confidence level correlation between beryllium microstructure and associated mechanical properties.

7

An additional motivation for examining these materials is
provided by the fact that both the HIP-50 and the X-520 grades of
beryllium show macro-mechanical properties which are substantially
superior to those of the I-400 grade (used currently in inertial
devices) while possessing a much lower level of beryllium oxide, BeO.
This latter feature allows the X-520 and HIP-50 grades to be fabricated
to a better surface finish than is possible with I-400. Micromechanical
data obtained as part of this effort has shown that these two beryllium
grades are also equally (in the case of X-520) or more (in the case of
HIP-50) resistant to short-term microdeformation, with respect to I-400,
as indicated by the measured microyield strength values. It is,
therefore, clearly of interest to understand what makes these materials
superior to the presently used I-400 material. It is unfortunate,
however, that unlike I-400 beryllium which is produced in large
quantities, HIP-50 and X-520 were experimentally produced, both on a
laboratory scale -- the former by Kawecki-Berylco using hot isostatic
pressing of high purity beryllium powder and the latter by the Brush-
Wellman Co. using hot pressing of lower purity powder. Kawecki-Berylco
has since discontinued its beryllium business. Table I shows a
comparison of the several properties, as reported by the manufacturers,
of the three beryllium grades. It should be noted that I-400 contains
the highest level of chemical impurities and HIP-50 the least. Also to
be noted are the macromechanical properties of both the experimental
beryllium grades provided by the manufacturers; while comparing
favorably to each other, the HIP-50 and X-520 values are considerably
superior to those of I-400 beryllium.

## 4.2    Microyield and Macroyield Testing of HIP-50 and X-520 Samples

Tensile testing of these materials, after various special heat
treatments, was performed in both the micro ($1 \times 10^{-6}$ plastic strain)
and macro (0.2% plastic strain) regimes. The microyield data collected
on HIP-50 beryllium has been reported previously.[1] Additional macro-
yield observations made on HIP-50 and X-520 materials and microyield
evaluation of the X-520 beryllium grade are now reported in this study.

8

Table 1. Comparison of properties of X-520, HIP-50 and I-400 beryllium.

| Chemical Analysis | X-520 | HIP-50 | I-400 |
|---|---|---|---|
| BeO | 2.27% | 1.68% | 4.25% |
| Al | 200 ppm | 40 ppm | 1600 ppm |
| Si | 300 ppm | 40 ppm | 800 ppm |
| Fe | 600 ppm | 500 ppm | 2500 ppm |
| C | 1200 ppm | 290 ppm | 2500 ppm |
| Mg | 100 ppm | 20 ppm | 800 ppm |
| Ni | | 170 ppm | |
| Grain Size (Microns) | 5 | 9 | 10 |
| Mechanical Properties | | | |
| U.T.S (lb/in$^2$) | 73,000 | 81,000 | 50,000 |
| Y.S. (lb/in$^2$) | 56,000 | 63,000 | — |
| Elongation (%) | 2 to 5% | 4% | <1% |

[Details on the experimental procedures and apparatus used for obtaining the microyield data are discussed in Reference (3).] The macroyield measurements were made in conventional manner using an Instron testing machine. It was hoped that a correlation might exist between the micro- and macroyield behaviors and these experiments were performed to determine if such a correlation indeed existed. The measurements were made on samples both in the as-pressed as well as in the heat treated condition. Additionally, with the X-520 material, two sets of samples were evaluated (one set each belonging to the longitudinal and the transverse directions of pressing, respectively) whereas only one set was examined for the HIP-50 material, principally because of a shortage of material availability and also because this grade of beryllium is very isotropic, having been produced by the hot isostatic pressing (HIP) technique. X-520, on the other hand, is produced by the more conventional uniaxial hot pressing process and is therefore expected to display some anistropy.

Notable differences in behavior were seen for these materials in their response to heat treatment as well as in their measured tensile properties. [The heat treatments that were used, as indicated elsewhere[1] were the result of studies in Reference (5).] The HIP-50, as received, showed a macroyield stress which was comparable to I-400 but its microyield stress was 60 percent higher (~17 kpsi for HIP-50 versus ~10 kpsi for I-400). Of the three heat treatments that were used, an aging treatment of 600°C/100 hours was the most effective, raising the macroyield by 26 percent to 70.5 kpsi. However, the microyield increase was much greater, 59 percent, to 27 kpsi. Heat treatments at 870°C, followed by a step aging treatment, and at 1050°C, followed by aging at 370°C, gave improvements of approximately 20 percent and 2 to 4 percent, respectively, for yield stress measurements in both regimes.

On the other hand, tensile testing of the X-520 grade beryllium in the "as received" condition showed values of macro- and microyield stress which barely met the accepted specifications for I-400. These

numbers were virtually unaffected by any of the heat-treatments,
although there was an apparent slight improvement imparted by the
600°C/100 hour aging exposure. All of the collected data is shown in
Tables 2, 3, and 4. Comparison of the X-520 results with those for
HIP-50 and I-400 suggests the importance of factors, other than the
grain size, such as the presence of dispersed phases, including
precipitates, or small quantities of dissolved contaminants in
determining the microyield behavior of the material. It may be
significant that the silicon content of the X-520 was higher than in the
HIP-50. This contaminant was found by NBS in their survey to correlate
with reduced strength.[6] The elevated silicon, in the absence of an
offsetting strengthening by a dispersed BeO phase, may be the basis for
the low tensile values shown for X-520 here.

Table 2.  Summary of microyield data* on
Brush Wellman X-520 and KBI HIP-50.

| Microyield Strength ($lb/in^2$) | | | |
|---|---|---|---|
| Specimen Condition | X-520 | | HIP-50 |
| | Longitudinal | Transverse | |
| As Received | 8000 | 8600 | 17,000 |
| HT1 | 8300 | 9000 | 27,000 |
| HT2 | 8100 | 7900 | 17,700 |
| HT3 | 9600 | 8200 | 20,800 |

* Microyield data is for $1 \times 10^{-6}$ offset

HT1:  HIP + 600°C, 100 h

HT2:  HIP + 1055°C, 2 h solutionize, quench + 370°C, 24h,
       furnace cool

HT3:  HIP + 870°C, 2 h + slow cool and step age
       (750°C, 20 H + 720°C, 20 h + 695°C, 20 h, furnace cool)

11

Table 3. Tensile testing of HIP-50 beryllium.

| Sample Number | Dia., in. | Area, in.$^2$ | Gage Length | 0.2% Yield, lbs | Macroyield, lb/in.$^2$ | Microyield, lb/in.$^2$ | Ratio: Micro/ Macro | Heat Treatment |
|---|---|---|---|---|---|---|---|---|
| 3A | 0.245 | 0.0471 | 1.0 in. | 3,065 | 56,010 | 17,000 | $2.61 \times 10^{-1}$ | As Received |
| 5A | 0.245 | 0.0471 | 1.0 in. | 3,325 | 70,530 | 27,000 | $3.83 \times 10^{-1}$ | HT1 |
| 2A | 0.245 | 0.0471 | 1.0 in. | 2,690 | 57,060 | 17,700 | $3.10 \times 10^{-1}$ | HT2 |
| 3B | 0.245 | 0.0471 | 1.0 in. | 3,149 | 66,800 | 20,800 | $3.11 \times 10^{-1}$ | HT3 |

Table 4. Tensile testing of X-520 beryllium.

| Sample Number | Longit./ Transv. | Dia. in. | Area in.$^2$ | Gage Length | 0.2% Yield, lbs | Macro- Yield, lb/in$^2$ | Micro- Yield, lb/in$^2$ | Ratio: Micro/ Macro | Heat Treatment |
|---|---|---|---|---|---|---|---|---|---|
| 1 | L | 0.247 | 0.04792 | 1.0 in. | 2,550 | 53,220 | 8,000 | $1.50 \times 10^{-1}$ | As Received |
| 5 | T | 0.246 | 0.04753 | 1.0 in. | 2,590 | 54,490 | 8,600 | $1.57 \times 10^{-1}$ | As Received |
| 2 | L | 0.247 | 0.04792 | 1.0 in. | 2,475 | 51,650 | 8,300 | $1.61 \times 10^{-1}$ | HT1 |
| 6 | T | 0.2495 | 0.04889 | 1.0 in. | 2,700 | 55,220 | 9,000 | $1.63 \times 10^{-1}$ | HT1 |
| 3 | L | 0.236 | 0.04374 | 1.0 in. | 2,395 | 54,750 | 9,600 | $1.75 \times 10^{-1}$ | HT3 |
| 7 | T | 0.238 | 0.04449 | 1.0 in. | 2,335 | 52,490 | 8,200 | $1.56 \times 10^{-1}$ | HT3 |

13

As shown elsewhere,[1] even in the absence of the desired microcreep data for the materials whose correponding microyield testing has been accomplished, it has been possible to gain further insight into the implications of the data which have been obtained. In many cases, for low levels of strain such as those contemplated here, the stress-strain relationship can be expressed empirically as

$$\sigma = A\epsilon^n \text{ (for } \epsilon' \leqslant \epsilon \leqslant \epsilon'')$$

or

$$\log \sigma = n \log \epsilon + \log A$$

where

$\sigma$ = applied stress

$\epsilon$ = residual strain

$\epsilon', \epsilon''$ = assigned values of strain in the low strain regime

$n$ = strain exponent

$A$ = proportionality constant

If the stress-strain data are shown on a log-log plot the slope of the curve is therefore n, the strain exponent, which is believed to have physical significance related to the strain hardening processes in the material. Clearly, therefore, this quantity should have a strong relationship to the microcreep characteristics of the material, since a larger strain exponent implies the need for a larger stress to produce a given level of residual strain. However, because creep is a process occurring over an extended period of time, other time-dependent processes such as diffusion will also have an effect on the total observable creep phenomenon.

Log-log plots of the data obtained for HIP-50 and X-520 revealed wide variations in strain exponent between the two materials and among the heat treatments applied. The existence of differing slopes for the various stress-strain relationships of the different material types and conditions implies that the perceived relative merits of any two materials or heat treatments will change depending on the strain level at which they are compared. When it is considered that the $10^{-6}$ level is completely arbitrary, and that a completely different ranking of apparent value could be obtained by simply focusing on a different low level of strain, it is apparent that assessment of resistance to microplastic deformation must take into account such additional factors as the strain exponent.

Along with the consideration that a strain level of $10^{-6}$ is purely arbitrary, there is the recognition that if strains of ever-lower orders of magnitude are contemplated, one will be reached which is infinitesimally small. The strain level of $10^{-10}$ might be considered to be such a marginally detectable strain, and the stress value needed to produce such a minimal plastic deformation could be designated as the intrinsic strength of the material, or the threshold stress needed to effect the onset of plastic deformation.[7]

On the assumption that the measured values of low-regime stress-strain data are capable of extrapolation down to the $10^{-10}$ strain intercept, the data shown in Table 5 were determined. It should be noted, however, that in each instance only one sample was measured mainly because of material shortage. Even so, whereas the relative values obtained from the different heat treatment conditions for samples belonging to a given beryllium grade might be suspect (because only one sample was measured in each instance), the data clearly shows that substantial differences in microyield behavior do exist between the HIP-50 and the X-520 beryllium grades. HIP-50 shows a considerably larger MYS (and "intrinsic" strength) value and a substantially lower strain exponent, "n," value than does X-520. As mentioned earlier, the observed microcreep phenomenon is expected to depend on both the MYS and

15

the "n" values; therefore, the significance of these calculated values
will only be demonstrated once reliable microcreep data have been
collected on samples from these materials. A tension microcreep
measuring apparatus is being assembled at CSDL for this purpose. Its
design details and expected capabilities are discussed in a later
section of this report.

Table 5. "Instinsic strength" and strain exponent.

| Material/Heat Treatment | $\sigma$, $10^{-10}$, kpsi | n |
|---|---|---|
| HIP-50/As HIP | 1.3 | 0.28 |
| HIP-50/HT-1 | 1.9 | 0.28 |
| HIP-50/HT-2 | 2.8 | 0.20 |
| HIP-50/HT-3 | 0.9 | 0.34 |
| | | |
| X-520 L*/As received | 0.16 | 0.43 |
| X-520 T†/As received | 0.16 | 0.43 |
| X-520 L/HT-1 | 0.14 | 0.45 |
| X-520 L/HT-1 | 0.12 | 0.47 |
| X-520 L/HT-2 | 0.26 | 0.38 |
| X-520 T/HT-2 | 0.14 | 0.44 |
| X-520 L/HT-3 | 0.23 | 0.41 |
| X-520 T/HT-3 | 0.11 | 0.48 |

\* Longitudinal

† Transverse

## 4.3    Microstructure Evaluations

### 4.3.1  Optical Microscopy

Earlier work on HIP-50 material had shown that optical microscopy was of limited utility in determining the effects of the several heat treatments on microstructure.  Optical examination of the as-received and heat treated X-520 samples was, therefore, performed only from the view of observing the as received grain size and any subsequent changes in it that might have occurred from the heat treatments that were employed.  (As reported earlier for the HIP-50 materials,[1] all of the heat treatments on X-520 samples were also performed after sealing them under an argon partial pressure inside stainless steel containers. This avoided both a potential for furnace contamination as well as significant beryllium loss from the samples due to evaporation.)

In line with earlier observations on the HIP-50 materials, no appreciable changes in the X-520 grain size were observed from the different heat treatments that were employed.  The micrographs showing the respective grain sizes were obtained using differential phase contrast (Nomarski) microscopy and two of these are shown in Figure 1. Care was taken in the preparation of these samples since it was known that it is easy to introduce mechanical damage in the surface regions of these materials if extreme care is not exercised.  It was interesting to note from the micrographs in Figure 1 that the grain size of the X-520 is about 10 µm and, therefore, similar to that of HIP-50 and I-400 beryllium and not considerably smaller than these beryllium grades as was earlier believed from the data shown in Table 1.  The large differences in behavior observed between HIP-50 and X-520, given their somewhat comparable levels of oxygen, must, therefore, be related to microstructure effects stemming from the other differences in composition.
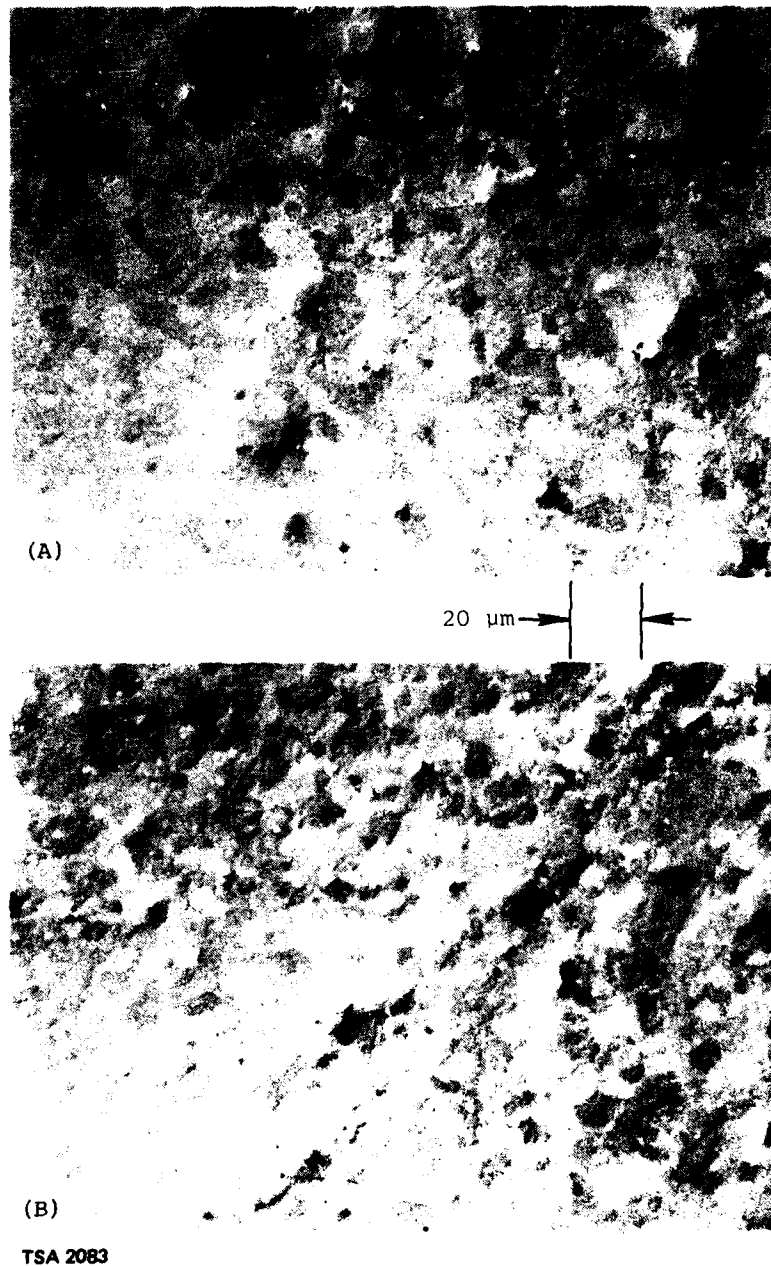
20 μm

Figure 1. Nomarski micrographs on X-520 samples.
(A) As received; (B) After HT 3.

18

## 4.3.2 Scanning Electron Microscopy (SEM)

SEM examination of fractured surfaces of several of the samples failed to show many significant topographical differences between the HIP-50 and the X-520 materials. Photographs obtained on fractured surfaces of these beryllium grades in the as-pressed (as-received) condition are shown in Figure 2. EDAX (energy dispersive x-ray analysis) of HIP-50 did not show any preferential segregation of the several low level impurity elements that are known to be present in this material. SEM examination of X-520, however, was somewhat more promising. A few regions were observed in this sample that appeared somewhat less crystalline than the bulk of the material. One such region is shown in Figure 3 at different magnifications. This region was analyzed and found to contain significantly larger quantities of Si and Al than did the surrounding material. Indications of a higher concentration of oxygen in this region were also present. The signal for Fe, in contrast, appeared to be no higher than background. X-ray maps obtained for the different elements showing their spatial distribution, at low magnification are shown in Figure 4. It was noted that some small particulates observed on the fractured sample surfaces (such as those in Figures 2 and 3) did not contain any elements that could be detected by the present apparatus (which constitute all the elements that are believed to be the major impurities in these beryllium grades).

## 4.3.3 X-Ray Diffraction Analysis

The amount of extraneous phases, composed presumably of the elements Fe, Al and Be in the beryllium samples are so small that their detection by the X-ray diffraction technique would not normally be expected. However, if a sufficiently pure narrow band of X-ray with small wave length, such as filtered $Cu_{K\alpha}$ radiation is used for diffraction of the beryllium sample, then very long time exposures can be used without darkening the photographic film. The absorption edge of beryllium being extremely large compared to the 1.54 Å $Cu_{K\alpha}$ radiation,

TSA 2084          20 μm ⊢———⊣  ⊢—————

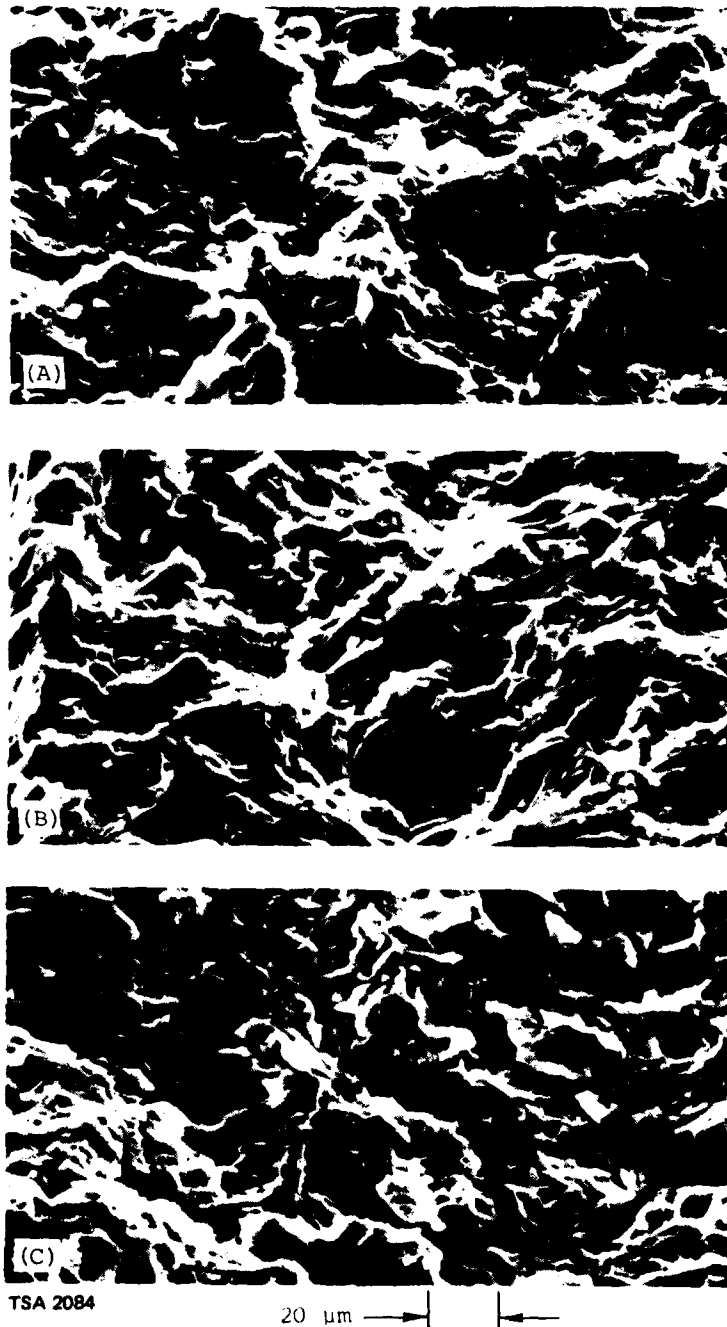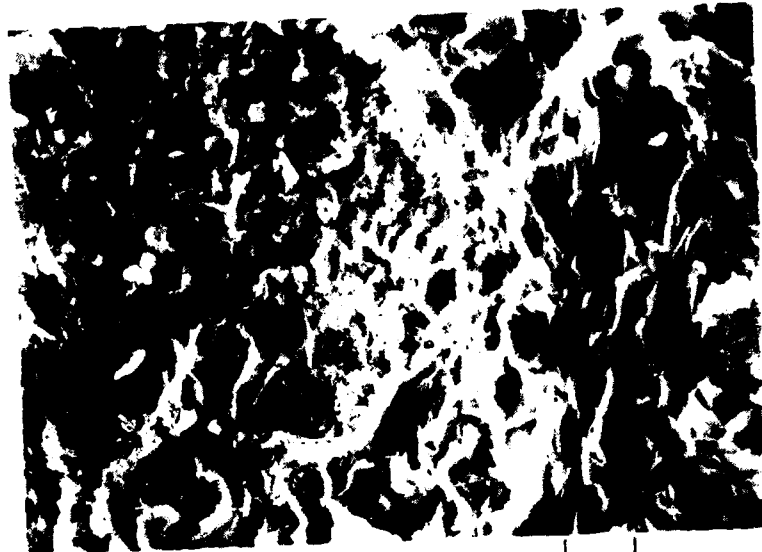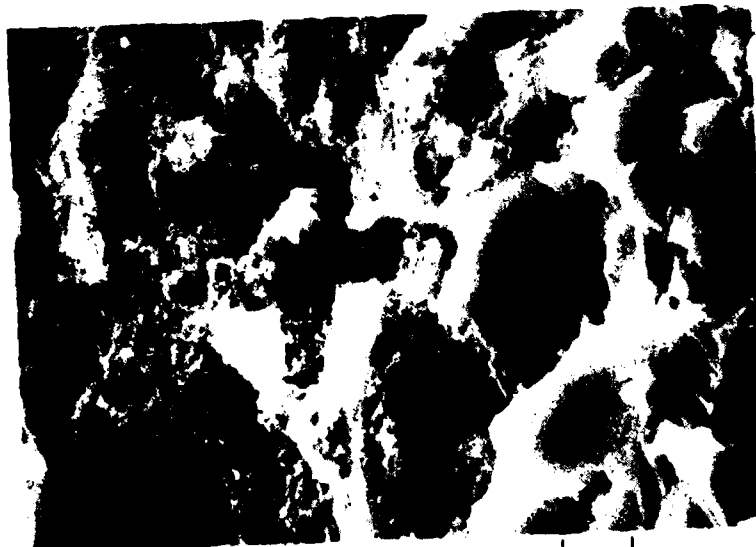Figure 2.  As-pressed fractured surfaces of (A) HIP-50;
           (B) X-520, transverse; and (C) X-520, longitudinal.
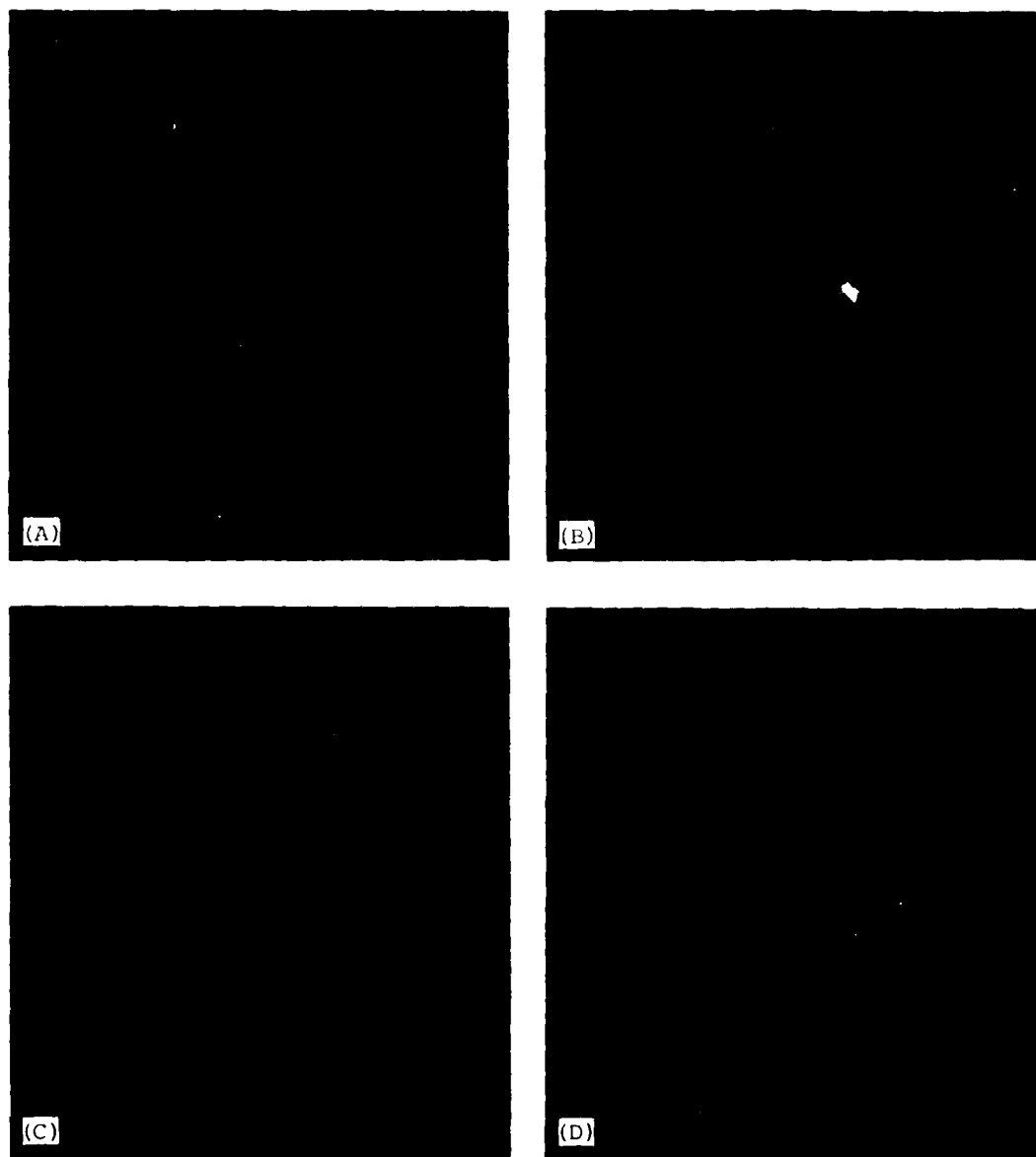           SEM examination.

20

20 μm

TSA 2085

5 μm

Figure 3.  Region observed in X-520 sample.
Different magnifications.

21

TSA 2086

Figure 4. X-ray maps of region shown in Figure 3 at low magnification. (A) Aluminum, Al; (B) Silicon, Si; (C) Oxygen, O; (D) Iron, Fe.

22

there is no fluorescence of the sample. The main cause of film darkening is thus not present. Very long time exposures for diffraction can therefore be used, which might then produce characteristic diffraction patterns of very minor amounts of second phases.

Based on the above reasoning, x-ray diffraction patterns were obtained using a Debye-Scherer camera. The x-radiation used was Ni-filtered Cu-radiation at 35 KV and 20 mA, and the exposure times were 21 to 24 hours for each sample. The samples examined were HIP-50 and X-520 grade beryllium in the as-received as well as the heat treated condition. The effects of the heat treatments were not noticable in the diffraction patterns. All four HIP-50 produced identical patterns, as did the X-520 group. But there was a distinct difference between the two groups with respect to the presence of diffraction lines from trace amounts of extraneous phase (or phases). In both groups of patterns, the beryllium diffraction lines were very strong and the BeO lines were of medium intensity. Very weak diffraction patterns were obtained of extraneous phases in the form of lines and wide bands, which were different for the two groups (HIP-50 and X-520), although identical within the groups. Therefore, only one set of diffraction data is presented for each group in Table 6, along with the data on some compounds obtained from the ASTM diffraction card file.

The very strong lines and the medium strength lines obtained from both categories of the metal are due to beryllium and its oxide respectively. Except for a couple of bands at very high 'd' spacings, all the other lines of HIP-50 are easily accounted for by Be and hexagonal BeO patterns. HIP-50 Be is therefore a higher purity metal than the X-520, although the latter appears to contain extremely small amounts of impurity.

Table 6. Diffraction data of HIP-50, X-520 along with various compounds from ASTM card files.

| HIP-50 | X-520 | Be | BeO | FeBe$_{11}$ | FeAl$_2$Be$_3$ | Be$_2$SiO$_4$ |
|---|---|---|---|---|---|---|
| d(Int) | d(Int) | d(Int) | d(Int) | d(Int) | d(Int) | d(Int) |
| 11.5(?) | 11.5 Band | | | 10.7(55) | | |
| 5.7(?) | 5-7 Band | | | | | 6.24(40) |
| | 3.66(VVW) | | | 5.36(65) | 3.73(50) | 3.67(75) |
| | | | | 3.57(100) | | |
| | | | | 3.39(25) | | |
| 3.15(VVW) | 3.15(VVW) | | | | 3.16(50) | 3.12(100) |
| | | | | 2.97(65) | | |
| | 2.52(W) | | | 2.53(50) | | 2.52(75) |
| 2.35(M) | 2.35(M) | | 2.35(91) | | | |
| 2.20(M) | 2.20(M) | | 2.19(61) | | 2.21(100) | |
| 2.10(M) | 2.09(M) | | 2.06(100) | | | |
| 1.99(VVS) | 1.99(VVS) | 1.98(30) | | | | |
| 1.80(VVS) | 1.80(VVS) | 1.79(25) | | | | |
| 1.74(VVS) | 1.75(VVS) | 1.73(100) | | | | |
| 1.61(W) | 1.61(W) | | 1.6(22) | | | |
| | 1.54(VW) | | | | | 1.53(7) |
| | | | | | | 1.50(VS) |
| | | 1.37(30) | | | | |
| 1.35(W) | 1.35(W) | 1.32(11) | | | | |
| 1.33(S) | 1.33(S) | | | | | |
| 1.24(W) | 1.24(W) | | 1.238(29) | | | |
| 1.15(S) | 1.15(S) | 1.15(9) | | | | |

In addition to the Be, BeO diffraction peaks and the two low angle broad bands obtained for both the samples, there are four additional lines in the X-520 patterns. Of the compounds $FeBe_{11}$, $FeAl_2Be_3$ and $Be_2SiO_4$ used for comparison, $Be_2SiO_4$ appears to give the best fit with all of these lines. Therefore, the impurity causing the diffraction peaks are assumed to be due to a presence of $Be_2SiO_4$ in the X-520 Be.

It should be remembered that SEM investigations of a freshly fractured X-520 surface, showed the presence of Si, Al, and O in an isolated spot, but, no evidence could be obtained for the presence of Fe. The presence of Si and O and the absence of Fe can be easily accounted for by the compound $Be_2SiO_4$. However, Al is not explained using this analysis. For the present, little significance is attached to the two broad bands appearing at 5.7 and 11.5 Å (indicative of an amorphous phase) since it is possible that the two bands may be a characteristic feature of the specific Debye Scherer camera that was used. Further TEM/STEM studies are planned on these materials.

# SECTION 5

## MICROCREEP ANALYTICAL STUDIES

The purpose of the analytical studies has been to apply the creep laws to gyro design, to try and give direction to the microcreep experiments from a design viewpoint and to support the experimental activities with a finite element analysis.

Previous reports (References 1,3,4) have shown that analysis of instrument trends due to microcreep, using finite element codes is feasible. However, the creep law used to demonstrate this feasibility was not based on reliable data. The form of law used was of power dependency on stress, linear with time. Recent data from NBS have best been fitted by a curve of the form

$$E_{ct} = E_{op} + A \ln \left(1 + \frac{t}{B}\right)$$

where

$E_{ct}$ = total creep strain

$A \& B$ = adjustable parameters

$E_{op}$ = instaneous plastic strain

$t$ = time

The data taken has been primarily in the range of 10-20 kpsi. Stresses in inertial components generally are limited to the 0-5 kpsi range. From this point of view it would be desirable for future tests to concentrate on tests in this area of applied stress. The stress dependence of $E_{op}$, and the constants A & B must be determined.

27

CSDL has also previously analysed a point loaded disc experiment underway at NBS. As results of this test become available, combined with further test specimen information, microcreep of critical beryllium instrument parts can be predicted with confidence.

# SECTION 6

## MICROCREEP TESTING APPARATUS

The scope of the work, including the $10^{-7}$ inch/inch microcreep capability, has warranted a very careful design of the apparatus which applies the tensile stress. It is for this reason that the most critical connection, that which couples the specimen to the pull rods, has been designed in-house. Care has been taken to choose materials of the proper strength, and where appropriate, those with the lowest contact resistance to allow proper alignment.

The underlying philosophy is that once the initial alignment is made, the only change to occur after a period of time should be to the structural dimensions of the specimen. In other words, no bending moment should be allowed initially to the specimen or allowed to occur through some unpredicted distortion in the load train components.

The coupling from the pull rods to the apparatus is made conventionally through knife edge couplings of 6000-lb capacity.

The apparatus consists of an Applied Test System's 10:1 ratio lever arm tester of 12,000-lb capacity. It has been modified to operate in the lever arm or dead load mode. This versatility is intended to maximize the accuracy of the instrument. In the case where the load is the lesser of 300 lb or 30 lb applied to the lever, the accuracy of the instrument falls off. It is best for this load range to switch to the dead load scheme with which loads can easily be applied down to 10 lb. These loading conditions correspond to 100 to 3000 $lb/in^2$ while in the dead load mode and 3000 to 10,000 $lb/in^2$ while in the lever arm mode.

For ease of operation as well as convenience, the apparatus is designed to convert from one to the other with minimal disturbance to the setup while maintaining the load train alignment. This is done by

leaving the devis coupling assembly to the lever arm intact and weighing down the lever arm onto the weight elevator at a setting which just unloads the train. At this point, one just needs to disengage the rest of the load train below the lower pull rod and attach the weight pan. The drawhead which normally serves to pull the lever arm to keep it horizontal can be used as a cruder but adequate weight elevator to relieve the tension in the dead load scheme.

The temperatures which will be used for testing will be 100°, 140° and 180°F. They will be provided by a cylindrical oven with holes at the top and bottom for the load train. Regulation is expected to be $\pm0.02$°F. Movement of the oven will be up and down for access to the micrometers. This is accomplished by a motor driven platform for smoothness. This also prevents one from accidentally bumping the specimen assembly.

Figure 5 is a schematic showing the specimen, its coupling to the pull rods, the capacitor plates and their accompanying signal measurement instruments. The method by which the capacitor plates are attached to the specimen has been discussed in a previous report.[1]

Figures 6 and 7 show the upper and lower capacitor plates respectively. The upper has three distinct regions with their own feed-through connector, thereby allowing for three separate readings which can be added or taken separately if one wants to check the alignment of the plates. This selection is made at the junction box.

The signal detection is to be routinely done through a General Radio 1615A capacitance bridge with the option of null detection or DC voltage output with the aid of a lock-in amplifier. The resolution of the instrument is expected to be well within the 0.1 μinch separation change desired.
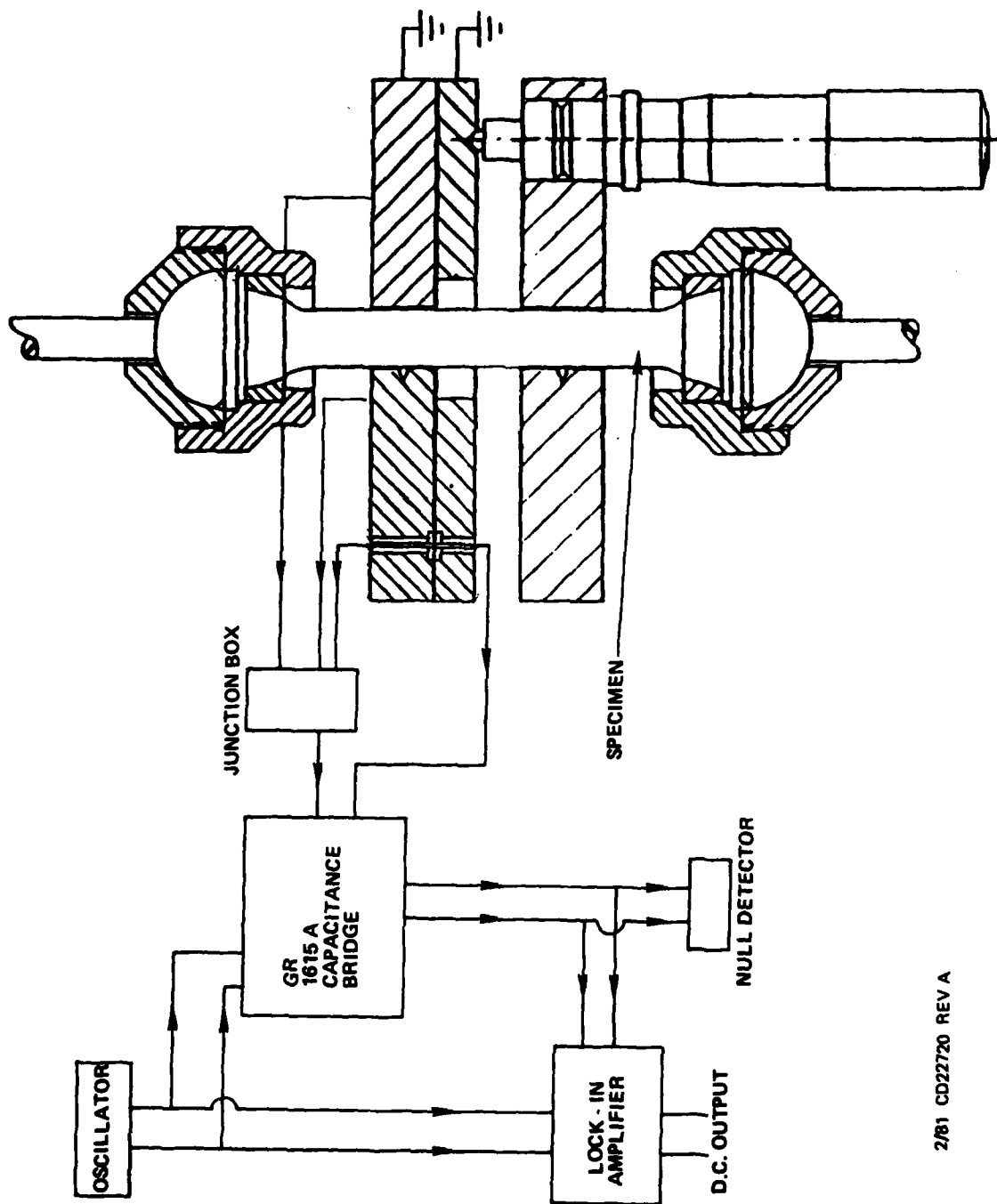
Figure 5. Capacitance signal detection of microcreep extensometer.

2/81 CD22720 REV A

31

GROUNDED
METALIZATION

VIEW Y-Y

SEE
DETAIL A

DETAIL A

"LOW" SIDE, CAPACITOR PLATE — Ni FILM
GROUNDED METALIZATION — BERYLLIUM
INSULATION — $Si_3N_4$ FILM
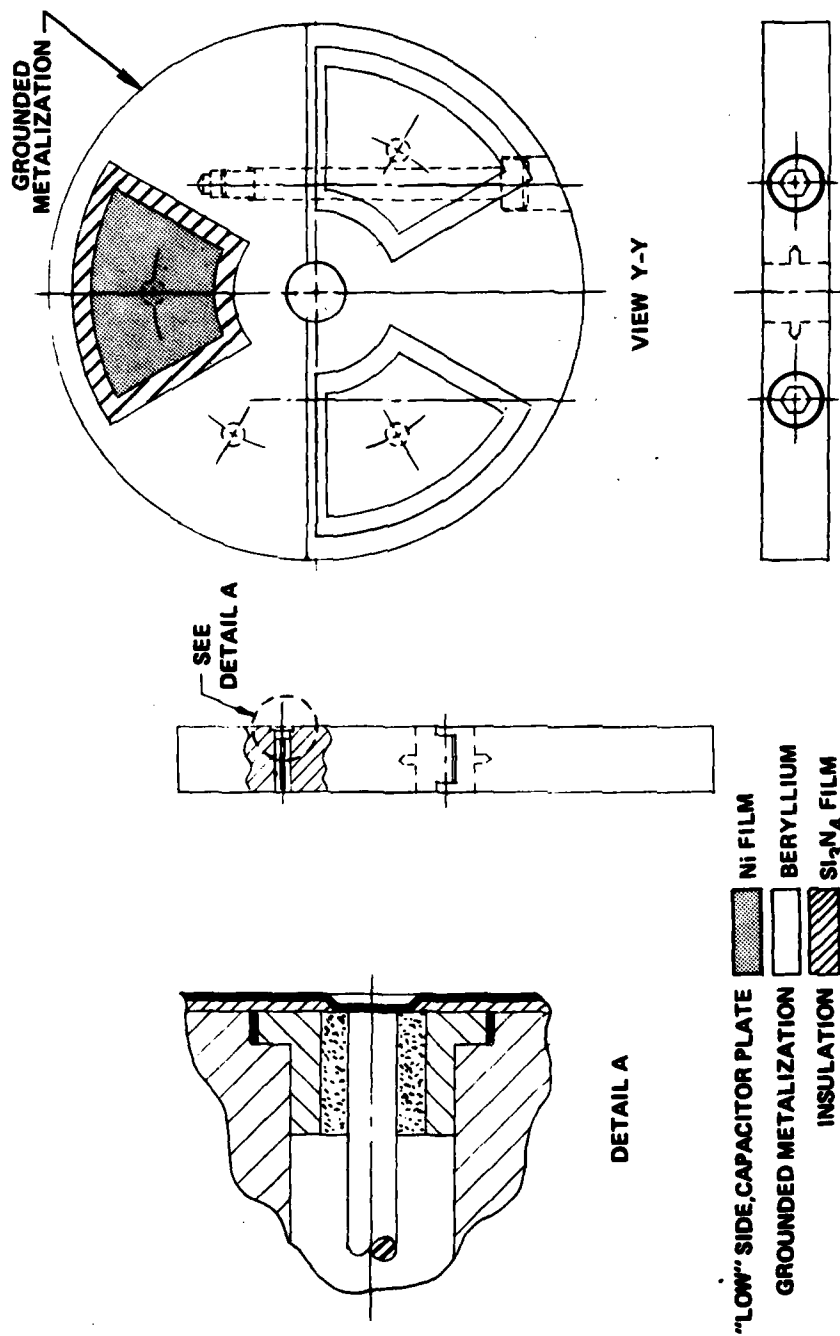
2/81 CD22675 REV A

Figure 6. Disk, capacitive.

32
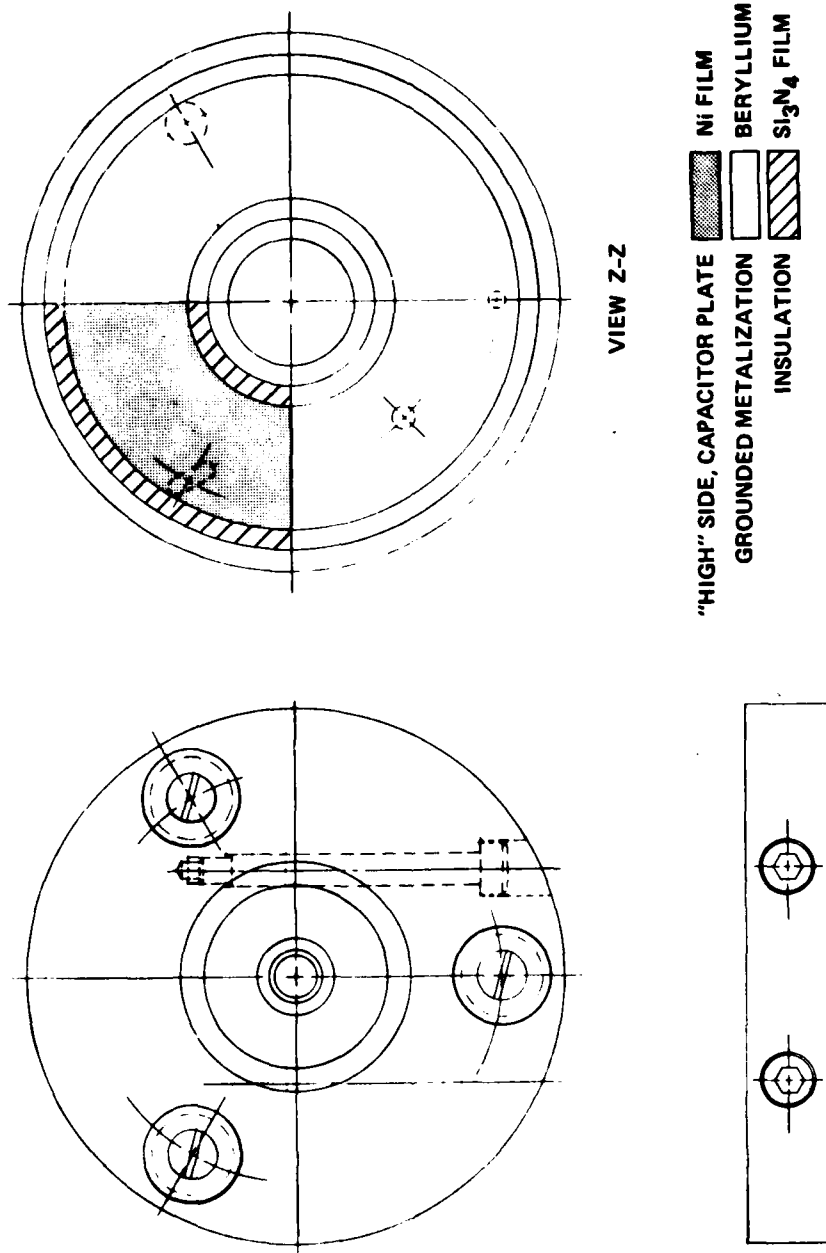
VIEW Z-Z

"HIGH" SIDE, CAPACITOR PLATE    Ni FILM

GROUNDED METALIZATION    BERYLLIUM

INSULATION    $Si_3N_4$ FILM

2/81 CD22673 REV A

Figure 7. Base disk, capacitive.

33

## References

(1) Kumar, K., J. McCarthy, F. Petri, and J. Wollam, _Materials Research for Advanced Inertial Instrumentation, Task 1: Dimensional Stability of Gyro Structural Materials_, The Charles Stark Draper Laboratory, Inc., Report No. R-1433, December 1980.

(2) Polvani, R., National Bureau of Standards (NBS), Gaithersburg, Maryland (private communication).

(3) McCarthy, J., and F. Petri, _Materials Research for Advanced Inertial Instrumentation, Task 1: Dimensional Stability of Gyro Structural Materials_, The Charles Stark Draper Laboratory, Inc., Report No. R-1231, September 1978.

(4) McCarthy, J., and F. Petri, _Materials Research for Advanced Inertial Instrumentation, Task 1: Dimensional Stability of Gyro Structural Materials_, The Charles Stark Draper Laboratory, Inc., Report No. R-1388, June 1980.

(5) Paine, R.M., and A.J. Stonehouse, _Investigation into Effects of Microalloying and Thermal Treatment on the Properties of Beryllium_, Final Report on Contract N60921-72-C-028, Brush-Wellman, Inc., Report BW-TR-549, Cleveland, Ohio, 1974.

(6) Polvani, R.S., B.W. Christ, and E.R. Fuller, Jr., "Beryllium Microdeformation Mechanisms" (private communication).

(7) Marschall, C.W., and R.E. Maringer, _Dimensional Instability - An Introduction_, Pergamon Press, 1977, p. 66.

BASIC DISTRIBUTION LIST

| ORGANIZATION | COPIES | ORGANIZATION | COPIES |
|---|---|---|---|
| Defense Documentation Center<br>Cameron Station<br>Alexandria, VA 22314 | 12 | Naval Air Propulsion Test Center<br>Trenton, NJ 08628<br>ATTN: Library | 1 |
| Office of Naval Research<br>Department of the Navy<br>800 N. Quincy Street<br>Arlington, VA 22217 | 1 | Naval Construction Battalion<br>Civil Engineering Laboratory<br>Port Hueneme, CA 93043<br>ATTN: Materials Division | 1 |
| ATTN: Code 471<br>Code 102<br>Code 470 | 1<br>1<br>1 | Naval Electronics Laboratory<br>San Diego, CA 92152<br>ATTN: Electron Materials<br>Sciences Division | 1 |
| Commanding Officer<br>Office of Naval Research<br>Branch Office<br>Building 114, Section D<br>666 Summer Street<br>Boston, MA 02210 | 1 | Naval Missile Center<br>Materials Consultant<br>Code 3312-1<br>Point Mugu, CA 92041 | 1 |
| Commanding Officer<br>Office of Naval Research<br>Branch Office<br>536 South Clark Street<br>Chicago, IL 60605 | 1 | Commanding Officer<br>Naval Surface Weapons Center<br>White Oak Laboratory<br>Silver Spring, MD 20910<br>ATTN: Library | 1 |
| Office of Naval Research<br>San Francisco Area Office<br>760 Market Street, Room 44702<br>San Francisco, CA 94102 | 1 | David W. Taylor Naval Ship<br>Research and Development Center<br>Materials Department<br>Annapolis, MD 21402 | 1 |
| Naval Research Laboratory<br>Washington, DC 20375 | | Naval Undersea Center<br>San Diego, CA 92132<br>ATTN: Library | 1 |
| ATTN: Code 6000<br>Code 6100<br>Code 6300<br>Code 6400<br>Code 2627 | 1<br>1<br>1<br>1<br>1 | Naval Underwater System Center<br>Newport, RI 02840<br>ATTN: Library | 1 |
| Naval Air Development Center<br>Code 302<br>Warminster, PA 18964<br>ATTN: Mr. F.S. Williams | 1 | Naval Weapons Center<br>China Lake, CA 93555<br>ATTN: Library | 1 |
| | | Naval Postgraduate School<br>Monterey, CA 93940<br>ATTN: Mechanical Engineering Dept. | 1 |

| ORGANIZATION | COPIES | ORGANIZATION | COPIES |
|---|---|---|---|
| Naval Air Systems Command | | NASA Headquarters | 1 |
| Washington, DC 20360 | | Washington, DC 20546 | |
| ATTN: Code 52031 | 1 | ATTN: Code RRM | |
| Code 52032 | 1 | | |
| | | NASA (216) 433-4000 | 1 |
| Naval Sea System Command | 1 | Lewis Research Center | |
| Washington, DC 20362 | | 21000 Brookpark Road | |
| ATTN: Code 035 | | Cleveland, OH 44135 | |
| | | ATTN: Library | |
| Naval Facilities Engineering | 1 | | |
| Command | | National Bureau of Standards | 1 |
| Alexandria, VA 22331 | | Washington, DC 20234 | |
| ATTN: Code 03 | | ATTN: Metallurgy Division | |
| | | Inorganic Materials Division | |
| Scientific Advisor | 1 | | |
| Commandant of the Marine Corps | | Director Applied Physics Laboratory | 1 |
| Washington, DC 20380 | | University of Washington | |
| ATTN: Code AX | | 1013 Northeast Fortieth Street | |
| | | Seattle, WA 98105 | |
| Naval Ship Engineering Center | 1 | | |
| Department of the Navy | | Defense Metals and Ceramics | 1 |
| Washington, DC 20360 | | Information Center | |
| ATTN: Code 6101 | | Battelle Memorial Institute | |
| | | 505 King Avenue | |
| Army Research Office | 1 | Columbus, OH 43201 | |
| P.O. Box 12211 | | | |
| Triangle Park, NC 27709 | | Metals and Ceramics Division | 1 |
| ATTN: Metallurgy and Ceramics | | Oak Ridge National Laboratory | |
| Program | | P.O. Box X | |
| | | Oak Ridge, TN 37380 | |
| Army Materials and Mechanics | 1 | | |
| Research Center | | Los Alamos Scientific Laboratory | 1 |
| Watertown, MA 02172 | | P.O. Box 1663 | |
| ATTN: Research Programs Office | | Los Alamos, NM 87544 | |
| | | ATTN: Report Librarian | |
| Air Force Office of Scientific | 1 | | |
| Research | | Argonne National Laboratory | 1 |
| Bldg. 410 | | Metallurgy Division | |
| Bolling Air Force Base | | P.O. Box 229 | |
| Washington, DC 20332 | | Lemont, IL 60439 | |
| ATTN: Chemical Science Directorate | | | |
| Electronics and Solid State | | | |
| Sciences Directorate | | | |

| ORGANIZATION | COPIES | ORGANIZATION | COPIES |
|---|---|---|---|
| Air Force Materials Laboratory<br>Wright-Patterson AFB<br>Dayton, OH 45433 | 1 | Brookhaven National Laboratory<br>Technical Information Division<br>Upton, Long Island<br>New York 19973 | 1 |
| Library<br>Building 50, Rm. 134<br>Lawrence Radiation Laboratory<br>Berkeley, CA | 1 | ATTN: Research Library<br><br>Office of Naval Research<br>Branch Office<br>1030 East Green Street<br>Pasadena, CA 91106 | 1 |

## SUPPLEMENTARY DISTRIBUTION LIST

Dr. Bruce W. Christ
Division 562
National Bureau of Standards
325 S. Broadway
Boulder, CO  80303

Dr. Robert S. Polvani
Room B-120, Materials Bldg.
National Bureau of Standards
Washington, DC  20234

Dr. A.W. Ruff, Jr.
National Measurement Laboratory
National Bureau of Standards
Washington, DC  20234

Dr. Robert Hocken
Room B-104, Metrology Bldg.
National Bureau of Standards
Washington, DC  20234

Dr. Gilbert J. London
Code 2023
Naval Air Development Center
Warminster, PA  18974

Professor G.S. Ansell
Rensselaer Polytechnic Institute
Dept. of Metallurgical Engineering
Troy, NY  12181

Professor J.B. Cohen
Northwestern University
Dept. of Material Sciences
Evanston, IL  60201

Professor M. Cohen
Massachusetts Institute of Technology
Department of Metallurgy
Cambridge, MA  02139

Professor J.W. Morris, Jr.
University of California
College of Engineering
Berkeley, CA  94720

Professor O.D. Sherby
Stanford University
Materials Sciences Division
Stanford, CA  94300

Dr. E.A. Starke, Jr.
Georgia Institute of Technology
School of Chemical Engineering
Atlanta, GA  30332

Professor David Turnbull
Harvard University
Division of Engineering and
  Applied Physics
Cambridge, MA  02139

Dr. D.P.H. Hasselman
Montana Energy and MHD Research
  and Development Institute
P.O. Box 3809
Butte, MT  59701

Dr. L. Hench
University of Florida
Ceramics Division
Gainesville, Fl  32601

Dr. J. Ritter
University of Massachusetts
Department of Mechanical Engineering
Amherst, MA  01002

Professor G. Sines
University of California, Los Angeles
Los Angeles, CA  90024

Director
Materials Sciences
Defense Advanced Research Projects
  Agency
1400 Wilson Boulevard
Arlington, VA  22209

Professor H. Conrad
University of Kentucky
Materials Department
Lexington, KY  40506

Dr. A.G. Evans
Dept. Material Sciences and
  Engineering
University of California
Berkeley, CA  94720

Professor H. Herman
State University of New York
Materials Sciences Division
Stoney Brook, NY  11794

Professor J.P. Hirth
Ohio State University
Metallurgical Engineering
Columbus, OH  43210

Professor R.M. Latanision
Massachusetts Institute of Technology
77 Massachusetts Avenue
Room E-19-702
Cambridge, MA  02139

Dr. Jeff Perkins
Naval Postgraduate School
Monterey, CA  93940

Dr. R.P. Wei
Lehigh University
Institute for Fracture and
  Solid Mechanics
Bethlehem, PA  18015

Professor H.G.F. Wilsdorf
University of Virgini
Department of Materials Science
Charlottesville, VA  29903

Mr. Robert C. Fullerton-Batten
Kawecki Berylco Industries, Inc.
P.O. Box 1462
Reading, PA  19603

Mr. Norman Pinto
Kawecki Berylco Industries, Inc.
P.O. Box 1462
Reading, PA  19603

A.G. Gross
Mechanical Metallurgy Unit
Autonetics, Inc.
Anaheim, CA

A.J. Stonehouse
The Brush Beryllium Co.
Cleveland, OH

C.W. Marschall
Columbus Laboratories
Battelle Memorial Institute
Columbus, OH

R.E. Maringer
Columbus Laboratories
Batelle Memorial Institute
Columbus, OH

J.E. Hanafee
Lawrence Livermore Laboratory
University of California
Livermore, CA  94550

Professor J. Van der Sande
Massachusetts Institute of Technology
Room 13-5025
Cambridge, Massachusetts  02139

Dr. Phil Clarkin
Metallurgy and Ceramics
Office of Naval Research
6th Floor, Room 619
800 N. Quincy Street
Arlington, VA  22217

Mr. George Keith
Kawecki Berylco Industries, Inc.
P.O. Box 1462
Reading, PA   19603

Mr. Bruce Borchardt
Room B-104, Metrology Bldg.
National Bureau of Standards
Washington, DC   20234

Dr. R.F. Karlak
Lockheed Missiles & Space Co.
3251 Hanover Street
Palo Alto, California   94304

Mr. Tom Charlton
Room B-104, Metrology Bldg.
National Bureau of Standards
Washington, DC   20234

Dr. James Marder
Brush-Wellman Co.
17876 Saint Claire Avenue
Cleveland, Ohio   44110

Dr. J. Smugeresky
Sandia National Laboratories
Livermore, California   94550

# DAT FILM